
On the acoustooptic efficiency of $\text{Pb}_2\text{P}_2\text{Se}_6$ crystals. Acoustic and thermal studies

¹ Mys O., ¹ Martynyuk-Lototska I., ^{1,2} Kostruba A. M., ³ Grabar A. and ¹ Vlokh R.

¹ Institute of Physical Optics, 23 Dragomanov St., 79005 Lviv, Ukraine, e-mail: vlokh@ifp.lviv.ua

² Lviv Academy of Commerce, 9 Samchuk St., 79011 Lviv, Ukraine, e-mail: amkostr@lac.lviv.ua

³ Institute for Solid State Physics and Chemistry, Uzhgorod National University, 54 Voloshyn St., 88000 Uzhgorod, Ukraine, e-mail: inpcss@univ.uzhgorod.ua

Received: 30.08.2012

Abstract. The acoustooptic properties of $\text{Pb}_2\text{P}_2\text{Se}_6$ crystals have been analysed on the basis of acoustic wave velocities, refractive indices and thermal expansion studies. The velocities of longitudinal and transverse acoustic waves propagating along the principal crystallographic directions have been determined. The acoustooptic figure of merit for the $\text{Pb}_2\text{P}_2\text{Se}_6$ crystals was estimated by us turns out to be high enough. These crystals represent an efficient acoustooptic material that reveals temperature-stable performance characteristics.

Keywords: acoustooptic figure of merit, acoustic wave velocities, thermal expansion

PACS: 78.20.hb, 62.65.+k, 65.40.De

UDC: 535.42

1. Introduction

Solid solutions with a general chemical formula $(\text{Pb}_x\text{Sn}_{1-x})_2\text{P}_2(\text{S}_{1-y}\text{Se}_y)_6$ attract much attention of researchers due to their nontrivial nonlinear and ferroelectric properties. One of the most comprehensively studied materials of this family is $\text{Sn}_2\text{P}_2\text{S}_6$ crystals. They are characterised with rather high electrooptic coefficients ($r_{11} = 1.74 \times 10^{-10}$ m/V at the room temperature and $\lambda = 633$ nm light wavelength of [1, 2]), high enough Faraday coefficients, and are also known as an excellent photorefractive material [3, 4]. Besides, $\text{Sn}_2\text{P}_2\text{S}_6$ crystals are one of the most efficient acoustooptic materials. Their acoustooptic figure of merit (AOFM) is as high as $M_2 = 1.7 \times 10^{-12} \text{ s}^3/\text{kg}$ [5]. Substitution of sulphur ions by selenium ones in the solid solutions $\text{Sn}_2\text{P}_2(\text{Se}_x\text{S}_{1-x})_6$ results in lowering the acoustic wave velocities and so increasing AOFM [6]. However, the phase transition temperature ($T_C = 337$ K [6]) in the $\text{Sn}_2\text{P}_2\text{S}_6$ crystals is very close to the normal ambient conditions, thus causing instability of many parameters of these crystals, including the acoustooptic ones [6]. This problem seems to have its solution in using the compounds with predominant concentrations of lead ions, e.g., $\text{Pb}_2\text{P}_2\text{Se}_6$ crystals which undergo no structural phase transitions [6]. These monoclinic crystals (2/m symmetry point group [7]) are optically biaxial and transparent in the both visible and infrared spectral ranges. Their absorption edge corresponds to the light wavelength of 591 nm [7]. At the same time, the optical properties of $\text{Pb}_2\text{P}_2\text{Se}_6$, including the acoustooptic ones, have not yet been studied. contrary to the $\text{Sn}_2\text{P}_2\text{S}_6$ crystals. The present work is devoted to

the analysis of acoustooptic properties of $\text{Pb}_2\text{P}_2\text{Se}_6$ on the basis of experimental studies of their acoustic wave velocities, refractive indices and thermal expansion, in comparison with other crystal of this family.

2. Experimental methods

The $\text{Pb}_2\text{P}_2\text{Se}_6$ crystals were grown with a Bridgman technique at the Uzhgorod National University. Their principal crystallographic axes were determined using an X-ray diffraction technique. The lattice parameters at the room temperature and the atmospheric pressure are as follows: $a = 6.606 \text{ \AA}$, $b = 7.464 \text{ \AA}$, $c = 11.3346 \text{ \AA}$, and $\beta = 91.33 \text{ deg}$ (see [7]). The b axis is perpendicular to the symmetry mirror plane. Notice that the crystallographic coordinate system for the monoclinic crystals is not orthogonal, though the deviation from orthogonality of the a and c axes remains small enough [7]. Taking into account this fact, we can refer to the crystallographic coordinate system as orthogonal one, were the indices of the appropriate axes are labelled as $a = 1$, $b = 2$, $c = 3$.

The velocities of longitudinal and transverse ultrasonic waves were measured with a standard pulse-echo overlap method [8] at $T = 290 \text{ K}$. These waves have been excited in our samples with the aid of a piezoelectric transducers made of LiNbO_3 plates of different crystallographic orientations (the resonance frequency being $f = 10 \text{ MHz}$, the bandwidth $\Delta f = 0.1 \text{ MHz}$, and the acoustic power $P_a = 1 \dots 2 \text{ W}$). Elastic stiffness coefficients of the $\text{Pb}_2\text{P}_2\text{S}_6$ crystals were calculated using a known Christoffel equation. Since the crystals belong to the monoclinic symmetry group, their elastic stiffness tensor includes 13 nonzero independent elastic coefficients C_{ij} . However, strict and simple enough relations among the acoustic wave velocities and the elastic coefficients are available only for the four components:

$$C_{22} = \rho v_{22}^2, \quad C_{44} = \rho v_{32}^2, \quad C_{66} = \rho v_{12}^2 \quad \text{and} \quad C_{46} = ((\rho v_{21}^2 - \rho v_{23}^2)^2 - (C_{44} - C_{66})^2)^{1/2}, \quad (1)$$

where ρ is the crystal density and v_{ij} the acoustic wave velocity. Here index i corresponds to the propagation direction of the acoustic wave and j to the direction of its polarisation. All the other coefficients are linked with the acoustic velocities by much more complicated relations (see [9, 10]). In order to determine all of these coefficients, it is necessary to measure the velocities of quasi-longitudinal (QL) and quasi-transverse (QT) ultrasonic waves for at least six different directions ([100], [010], [001], [110], [101], and [011]).

The average refractive indices were determined with an ellipsometric technique, using the reflection experimental geometry at the wavelength of 632.8 nm . Temperature dependences of the relative elongations ($\Delta L_i / L_j^0 = (L_i - L_i^0) / L_j^0$, with L_i^0 and L_j^0 denoting the initial linear size of sample along the i axis and L_i its thermally induced size) were measured using an automated quartz dilatometer. The temperature was scanned in the cooling run with the rate of about 0.1 K/min . The accuracy of temperature determination was about 0.05 K .

For the monoclinic crystals, the tensor of thermal expansion coefficients, written in the crystallographic coordinate system, includes four independent components: α_{11} , α_{22} , α_{33} , and α_{13} . These coefficients are defined as

$$\alpha_{ij} = \frac{\partial(\Delta L_i / L_j)}{\partial T}. \quad (2)$$

Notice that the crystallographic coordinate system does not represent the eigen system for the thermal expansion tensor. Besides, latter coordinate system rotates around the crystallographic b axis while the temperature changes. In our experiments we were able to determine the diagonal components α_{11} , α_{22} , and α_{33} of the thermal expansion coefficients. The error of determination of the thermal expansion coefficients was about $\pm 10^{-5}$.

All of the measurements were performed using a single-crystalline $\text{Pb}_2\text{P}_2\text{S}_6$ plate, with the faces perpendicular to the principal crystallographic directions. The dimensions of our sample were $5.01 \times 6.02 \times 4.96 \text{ mm}^3$.

3. Results and discussion

The temperature dependences of the relative elongations measured along the directions a , b and c are presented in Fig. 1. As seen from Fig. 1, the relative elongations increase almost linearly with increasing temperature. The temperature dependences of the tensor components α_{ij} shown in Fig. 2 have been calculated using Eq. (2). It is clear that all the thermal expansion coefficients are positive and almost temperature-independent.

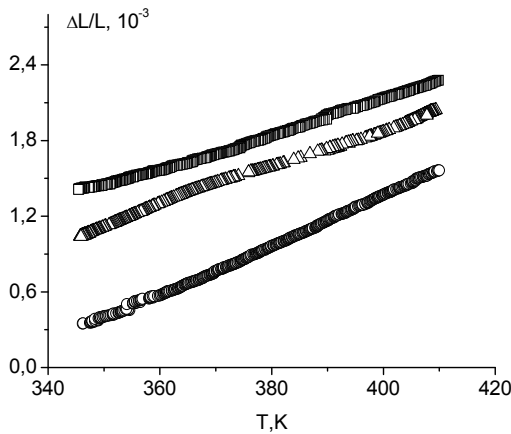


Fig. 1. Temperature dependences of relative elongations for the $\text{Pb}_2\text{P}_2\text{S}_6$ crystals measured along the principal crystallographic axes a (open triangles), b (open circles), and c (open squares).

Let us consider the acoustic properties of the $\text{Pb}_2\text{P}_2\text{S}_6$ crystals. The acoustic wave velocities referred to the crystallographic system are presented in Table 1. The lowest velocity ($v_{35} = 1426 \pm 70 \text{ m/s}$) is peculiar for the quasi-transverse wave that propagates along the $[101]$ direction and has polarisation parallel to $[\bar{1}01]$. Therefore the substitution of lead by tin in the solid solutions $(\text{Pb}_x\text{Sn}_{1-x})_2\text{P}_2\text{S}_6$ does not affect significantly the acoustic wave velocities. However, the simultaneous substitution of lead by tin and selenium by sulphur leads to notable changes in the acoustic velocities.

Basing on the results obtained above and solving the Christoffel equation, we have calculated the tensorial elastic stiffness coefficients C_{22} , C_{44} , C_{66} and C_{46} . Their mean values are $C_{22} = 43.59 \times 10^9 \text{ N/m}^2$, $C_{66} = 23.37 \times 10^9 \text{ N/m}^2$, $C_{44} = 14.88 \times 10^9 \text{ N/m}^2$, and $C_{46} = 2.0 \times 10^9 \text{ N/m}^2$.

Since the photoelastic coefficients p_{ijkl} for the $\text{Pb}_2\text{P}_2\text{S}_6$ crystals are unknown, we cannot determine rigorously the corresponding AOFM value. However, we can present the coefficient M_2 for $\text{Pb}_2\text{P}_2\text{S}_6$ as $M_2 = Kp^2$ (with the K coefficient defined according to $K = n^6 / \rho v^3$ and p the efficient value of the photoelastic coefficient) and compare it with the same value for the $\text{Sn}_2\text{P}_2\text{S}_6$

crystals. The AOFM was estimated from comparison of the K coefficient that corresponds to the acousto-optic interaction of light with the slowest longitudinal and transverse acoustic waves in $\text{Pb}_2\text{P}_2\text{Se}_6$ with that of the $\text{Sn}_2\text{P}_2\text{S}_6$ crystals.

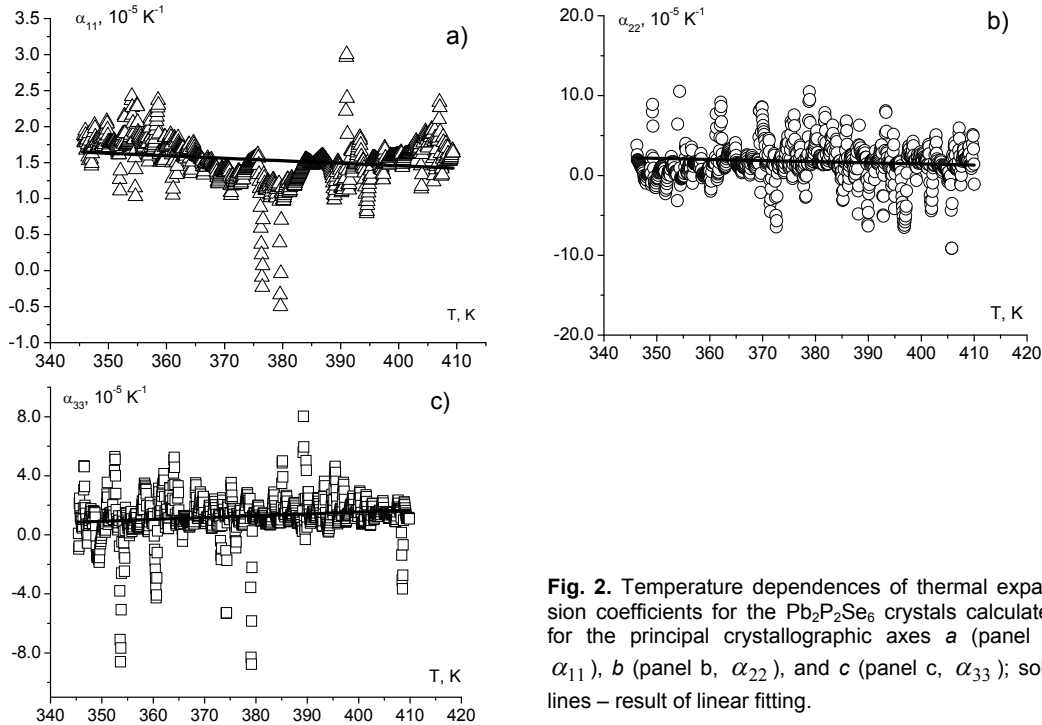


Fig. 2. Temperature dependences of thermal expansion coefficients for the $\text{Pb}_2\text{P}_2\text{Se}_6$ crystals calculated for the principal crystallographic axes a (panel a, α_{11}), b (panel b, α_{22}), and c (panel c, α_{33}); solid lines – result of linear fitting.

Table 1. Acoustic wave velocities for the $\text{Pb}_2\text{P}_2\text{Se}_6$, $\text{Sn}_2\text{P}_2\text{Se}_6$ [6] and $\text{Sn}_2\text{P}_2\text{S}_6$ [11] crystals ($T = 290$ K).

Direction of propagation	Direction of polarisation	Acoustic wave velocity in $\text{Pb}_2\text{P}_2\text{Se}_6$, m/s	Acoustic wave velocity in $\text{Sn}_2\text{P}_2\text{Se}_6$, m/s	Acoustic wave velocity in $\text{Sn}_2\text{P}_2\text{S}_6$, m/s
[100]	[100]	2922±20	2550	3550
[010]	[010]	2658±40	2680	3210
[001]	[001]	2783±80	2760	3635
[100]	[010]	1946±30	1920	2500
[100]	[001]	1861±40	1830	2335
[010]	[100]	1956±30	–	2480
[010]	[001]	1560±80	1690	2100
[001]	[100]	1868±30	–	2420
[001]	[010]	1553±40	–	2115
[101]	$[\bar{1}01]$	1426±30	–	1500
[101]	[010]	1700±130	–	–

As already mentioned for the case of $\text{Pb}_2\text{P}_2\text{Se}_6$, here the slowest transverse acoustic wave propagates in the ac plane along the crystallographic direction [101] and has the polarisation parallel to $[\bar{1}01]$. The relevant acoustic wave velocity is equal to 1426 ± 30 m/s. Using the known

value $\rho = 6170 \text{ kg/m}^3$ [7] and our data $n = 2.85$ and we obtain the AOFM equal to $M_2 = 2.295 \times 10^{-11} \text{ p}^2 \text{ s}^3/\text{kg}$. On the other hand, the AOFM characterising acoustooptic interaction with the slowest acoustic wave in $\text{Sn}_2\text{P}_2\text{S}_6$ is equal to $M_2 = 7.44 \times 10^{-11} \text{ p}^2 \text{ s}^3/\text{kg}$, where the values $n \approx 3$, $v = 1400 \text{ m/s}$, $\rho = 3570 \text{ kg/m}^3$ [5, 12] have been taken. As is seen from these results, the AOFM for $\text{Pb}_2\text{P}_2\text{Se}_6$ should be high enough, only approximately three times smaller than that for the $\text{Sn}_2\text{P}_2\text{S}_6$ crystals, provided that the effective photoelastic coefficient remains almost the same ($\sim 524 \times 10^{-15} \text{ s}^3/\text{kg}$).

Finally let us estimate the efficiency of acoustooptic interaction with the slowest longitudinal acoustic wave in $\text{Pb}_2\text{P}_2\text{Se}_6$. It is seen from Table 1 that the slowest longitudinal waves for the both $\text{Pb}_2\text{P}_2\text{Se}_6$ and $\text{Sn}_2\text{P}_2\text{S}_6$ correspond to the crystallographic direction b . Thus, the conditions of optimal acoustooptic interactions in the both crystals are the same. Then the AOFM for the $\text{Pb}_2\text{P}_2\text{Se}_6$ crystals would be equal to $M_2 = 4.635 \times 10^{-12} \text{ p}^2 \text{ s}^3/\text{kg}$. Under the same conditions, we have $M_2 = 6.174 \times 10^{-12} \text{ p}^2 \text{ s}^3/\text{kg}$ for $\text{Sn}_2\text{P}_2\text{S}_6$, which is only 1.33 times larger than that for the $\text{Pb}_2\text{P}_2\text{Se}_6$ crystals. Hence, the $\text{Pb}_2\text{P}_2\text{Se}_6$ crystals might be considered as a very efficient acoustooptic material when used in the visible or infrared spectral ranges.

4. Conclusions

On the basis of our studies for the acoustic wave velocities, the index of refraction and the thermal expansion in $\text{Pb}_2\text{P}_2\text{Se}_6$, one can conclude that these crystals may be referred to as an efficient acoustooptic material. Moreover, they reveal temperature-stable characteristics. The AOFM estimated for these crystals in the case of interaction with the slowest acoustic wave can be as high as $\sim 524 \times 10^{-15} \text{ s}^3/\text{kg}$.

We have also determined some of the components of the elastic stiffness tensor and the components of their thermal expansion tensor. It has been found that the thermal expansion coefficients are small enough and remain almost temperature-independent in the temperature range under study. We have also revealed that the substitution of tin ions by the lead ones in the solid solutions $(\text{Pb}_x\text{Sn}_{1-x})_2\text{P}_2\text{Se}_6$ causes no significant changes in the velocities of acoustic waves propagating along the principal crystallographic directions.

References

1. Vlokh R, Vysochanskii Yu, Grabar A, Kityk A and Slivka V, 1984. Electrooptic effect in $\text{Sn}_2\text{P}_2\text{S}_6$ ferroelectrics. *Izv. Akad. Nauk SSSR, Ser. Neorg. Mater.* **27**: 689–692.
2. Haertle D, Caimi G, Haldi A, Montemezzani G, Gunter P, Grabar A, Stoika I and Vysochanskii Yu, 2003. Electro-optical properties of $\text{Sn}_2\text{P}_2\text{S}_6$. *Opt. Commun.* **215**: 333–343.
3. Krupych O, Adamenko D, Mys O, Grabar A and Vlokh R, 2008. Faraday effect in $\text{Sn}_2\text{P}_2\text{S}_6$ crystals. *Appl. Opt.* **47**: 6040–6045.
4. Jazbinsek M, Montemezzani G, Gunter P, Grabar A, Stoika I and Vysochanskii Y, 2003. Fast near-infrared self-pumped phase conjugation with photorefractive $\text{Sn}_2\text{P}_2\text{S}_6$. *J. Opt. Soc. Amer. B.* **20**: 1241–1256.
5. Martynyuk-Lototska I, Mys O, Grabar A, Stoika I, Vysochanskii Y and Vlokh R, 2008. Highly efficient acoustooptic diffraction in $\text{Sn}_2\text{P}_2\text{S}_6$ crystals. *Appl. Opt.* **47**: 52–55.
6. Vysochanskii Y, Janssen T, Currat R, Folk R, Banyas J, Grigas J. and Damulionis V. Phase transitions in ferroelectric phosphorous chalcogenide crystals. Vilnius: Publishing House

- (2006).
7. Carpentier C and Nitsche R, 1974. Vapour growth and crystal data of the thio(seleno)-hypodiphosphates $\text{Sn}_2\text{P}_2\text{S}_6$, $\text{Sn}_2\text{P}_2\text{Se}_6$, $\text{Pb}_2\text{P}_2\text{S}_6$, $\text{Pb}_2\text{P}_2\text{Se}_6$ and their mixed crystals. *Mat. Res. Bull.* **9**: 401–410.
 8. Papadakis E, 1967. Ultrasonic phase velocity by the pulse-echo-overlap method incorporating diffraction phase corrections. *J. Acoust. Soc. Amer.* **42**: 1045–1051.
 9. Huntington H and Gangoli S, 1969. Ultrasonic measurement of the elastic constants of anthracene. *J. Chem. Phys.* **50**: 3844–3849.
 10. Prawer S, Smith T and Finlayson T, 1985. The room temperature elastic behaviour of CsH_2PO_4 . *Aust. J. Phys.* **38**: 63–83.
 11. Mys O, Martynyuk-Lototska I, Grabar A and Vlokh R, 2009. Acoustic and elastic properties of the $\text{Sn}_2\text{P}_2\text{S}_6$ crystals. *J. Phys.: Condens. Matter.* **21**: 265401.
 12. Mys O, Zapeka B, Martynyuk-Lototska I and Vlokh R, 2012. Elastic and acoustooptic properties of $\text{Sn}_2\text{P}_2\text{S}_6$ crystals: effect of ferroelastic phase transition. *Opt. Mater.* **35**: 168-174

Mys O., Martynyuk-Lototska I., Kostruba A.M., Grabar A. and Vlokh R., 2012. On the acoustooptic efficiency of $\text{Pb}_2\text{P}_2\text{Se}_6$ crystals. Acoustic and thermal studies. *Ukr.J.Phys.Opt.* **13**: 177 – 182.

***Анотація.** В даній роботі проаналізовані акустооптичні властивості кристалів $\text{Pb}_2\text{P}_2\text{Se}_6$ на основі досліджених швидкостей акустичних хвиль, показника заломлення та термічного розширення. Визначені швидкості поздовжніх і поперечних акустичних хвиль, які поширюються вздовж основних кристалографічних напрямків. Здійснено оцінку коефіцієнта акустооптичної якості кристалів $\text{Pb}_2\text{P}_2\text{Se}_6$, який виявився досить значним. Показано що дані кристали представляють ефективні акустооптичні матеріали з температурно-стабільними робочими характеристиками.*